

PHENOMENOLOGY OF SCATTERING MECHANISMS IN A TROPICAL FOREST THROUGH POLARIMETRIC SAR TOMOGRAPHY³

Mariotti d'Alessandro M ⁽¹⁾, Tebaldini S. ⁽¹⁾, Rocca F. ⁽¹⁾

⁽¹⁾ Politecnico di Milano, dipartimento di Elettronica Informazione e Bioingegneria, via Ponzio 34/5 Milano, mariotti.dalessandro@elet.polimi.it

ABSTRACT

In the recent years the estimation of the Above the Ground Biomass (AGB) is receiving a growing interest. For this reason many efforts have been made to relate together SAR signal and forest biomass. The main difficulty is represented by the large number of scattering mechanisms occurring when the wave impinges on the vegetation. Each one is affected in a different way by biomass and acquisition geometry or ground topography. Recently InSAR and TomoSAR techniques proved to be more effective than standard PolSAR algorithm. In this paper polarimetric TomoSAR is exploited in order to explore the contribution coming from the ground level. The fitting of a simple dihedral model gives a possible explanation for the need of multi baseline acquisitions when estimating the AGB.

1. INTRODUCTION

The recent choice of the Biomass mission by ESA is representative of the great interest in the estimation of the AGB. In the past years many algorithms have been developed with the objective of linking together SAR derived quantities and AGB. First attempts exploited the backscatter intensity only [1]; then polarimetric measurements was introduced improving the quality of the estimations [2]; the addition of multiple measurements opened the way to SAR interferometry [3]; more recently multiple baseline were added thus enabling SAR tomography [4]. The quality of the estimations had a significant boost when interferometric techniques began to be used rather than basing on backscattered power only. Such an improvement can be explained thanks the capability of attaining resolution along the vertical direction thus geometrically separating the scattering mechanisms (SMs).

This paper aims to understand the reason behind such improvement. It relies on the P-Band TropiSAR dataset [5] acquired in French Guyana. Tomography together with polarimetry are here exploited to achieve a comprehension of the dominant scattering mechanisms varying the elevation inside the vegetation layer. The former allows to focus on a certain height whereas the latter provides a characterization of the SM. It results that as long as the penetration is sufficient and the terrain is flat, the ground trunk double bounce mechanism is predominant. On one hand it follows that not to be deceived by the local topography interferometry is needed. On the other hand it appears

reasonable to relate the double bounce to the physical dimensions of the forest. The existence of such relationship is here explored.

This paper is organized as follows. In section 2 the algorithm to perform a model free tomography is explained; in section 3 the ground contribution is analyzed; section 4 introduces a model of the dihedral backscattering; in section 5 the dihedral features are explained thanks to an equivalent extinction model; finally in section 6 conclusion are drawn.

2. TOMOGRAPHIC PROCESSING

A single SAR survey takes the three dimensional scene under observation and projects it in a two dimensional space, namely the slant range and the azimuth plane. As long as the wave is able to penetrate into the medium under observation many contributions are received mixed up together. In particular the scattered waves coming from targets placed at the same distance from the radar sum coherently at the receiver. In a forest environment it basically means that the vertical direction is lost.

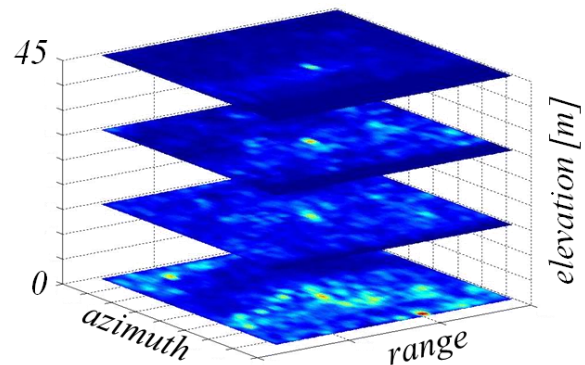


Figure 1. The Guyaflux tower as imaged by SAR tomography.

In order to back project each contribution to the elevation where it belongs many images are needed. In other words the joint processing of the multi baseline image stack is able to provide resolution along the vertical direction thus allowing an estimation of the backscatter coming from a specific height inside the vegetation layer. Mathematically the relationship between the vertical reflectivity profile and the multi baseline signal can be expressed as [6]:

$$y_n(r, x) = \int P(\xi, r, x) \exp\left(j \frac{4\pi}{\lambda r} b_n \zeta\right) d\zeta \quad (1)$$

Where ξ points out the cross range direction: orthogonal to the LOS and azimuth directions and related to the vertical. Equation 1 states that the signal in the n -th image represent a coefficient of the inverse Fourier transform of the vertical reflectivity profile $P(\xi, r, x)$. The imaged spatial frequency is determined by the n -th normal baseline. It follows that by taking a Fourier transform of the multi baseline signal an estimation of the vertical reflectivity profile can be obtained. If such processing is carried out for each polarimetric channel than fully polarimetric single look complex images associated with a certain height inside the vegetation layer can be computed.

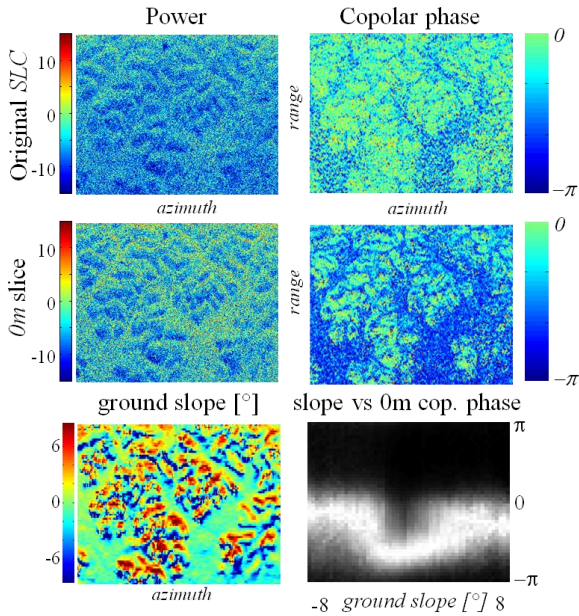


Figure 2. Top rows: backscattered power and copolar phase associated with the original slc image and with the tomographic image of the ground. Bottom row: ground slope along the ground range direction and histogram relating copolar phase to ground slope.

In order to refer height specifications to the forest layer regardless of the ground topography, the latter need to be identified and its height contribution compensated. In order to achieve such goal the approach described in [7] is followed. The main consequence is that the ground level is steered to 0m whichever the actual topography is present. After this processing step when referring to 0m or 15m it means *above the ground level*.

After the removal of the interferometric phases of the ground, the Fourier transform of the data stack has been carried out. A new data stack is thus obtained: each image refers to a different depth inside the vegetation layer. Fig. 1 shows a small part of such images in correspondence of the Guyaflux tower; a 55m tall metal tower surrounded by the tropical forest. Further details

on this processing steps can be found in [8].

3. ANALYZING THE GROUND LEVEL

Out of the several figures returned by SAR tomography the one associated with ground level has been here analyzed.

Fig. 2 shows the comparison between one of the 6 images of the multi baseline stack and the tomographic SLC image referred to the ground level. In order to properly interpret such results it must be kept in mind that high magnitudes of the copolar phase reveal the presence of a dihedral scattering mechanism [9]. It appears that the ground topography shapes the profile of the backscattered power. By observing the copolar phase it is clear that strong backscatter results whenever the ground is flat because the trunk and the ground act like a 90° dihedral. The histogram relating together ground slope and copolar phase allows to quantify the angle needed for the double bounce to vanish: three or four degrees are enough.

An interesting question is whether the double bounce can be related to any physical dimension of the forest and in turn to the AGB. Intuitively it could be related to the height of the trunks thus carrying useful information. In order to explore such possible relationship the double bounce mechanism has been analyzed more in detail. In particular the change in the histogram shown in fig. 2 with the look angle has been explored.

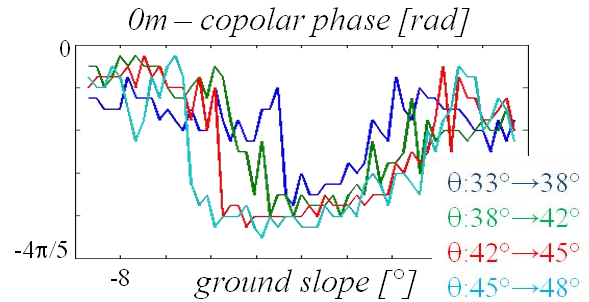


Figure 3. Shapes of histograms of the copolar phases varying the ground slope for different look angles.

Several histograms relating together copolar phase and ground slope have been computed; each one considering a limited range of look angles only. Then the ridge of each histogram has been considered and plotted in fig. 3. It appears that by increasing the look angle the width of the lobe associated with the double bounce mechanisms increases. In order to interpret such phenomenon a model was needed; it is presented in section 4.

4. MODELING THE DOUBLE BOUNCE

The model here considered for the dihedral backscatter dates back to the seventies [10]. It relates the received

power to the geometry of the dihedral and the look angle as well.

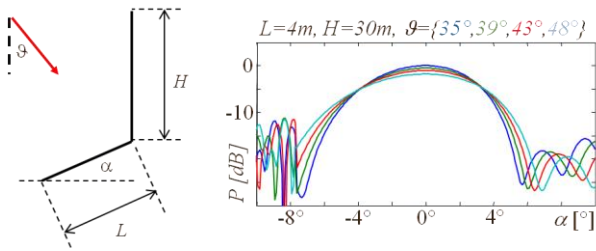


Figure 4. Leftmost panel: quantities needed to model the received power Rightmost panel: examples of received power according to the model.

As depicted in the leftmost panel of fig. 4 the model relies on: dihedral length (L) and height (H), ground slope (α) and look angle (ϑ). Thanks to geometrical and physical optics it allows to estimate the received power due to the double bounce mechanism. Examples of received power according to this model are shown in the rightmost panel of fig. 4. It can be observed that by increasing the look angle the lobe associated with the double bounce increases. Such behaviour follows the particular choice of parameters H , L and ϑ . In particular by setting $L \gg H$ this behaviour is reversed, that is the main lobe shrinks as the look angle increases.

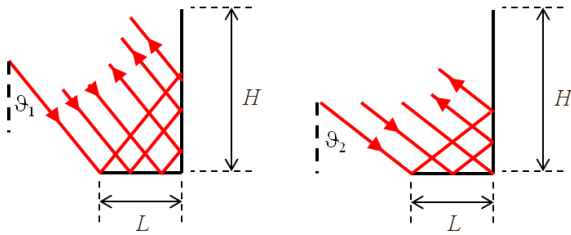


Figure 5. Optical rays bouncing on a dihedral whose height (H) is larger than its basis (L).

In order to understand why by setting either L greater than H or vice versa the behaviour of the main lobe changes, it is possible to refer to fig. 5. The limited length of the sides of the dihedral produces a partial illumination of one dihedral face. It follows that the effective dihedral area changes with the look angle. A smaller effective area means a wider lobe and vice versa. The main consequence of the partial illumination of one out of two faces of the dihedral is that the actual dimension of the partially illuminated face is not relevant in determining the backscatter. The fitting of the model is then achieved by choosing the proper L as H is not relevant.

Fig. 6 shows several plots of the width of the lobe associated with the double bounce mechanism varying the look angle. Any couple (ϑ , width) can be explained by either hypothesizing $L \gg H$ or $H \gg L$; by examining the trend these two situations can be distinguished.

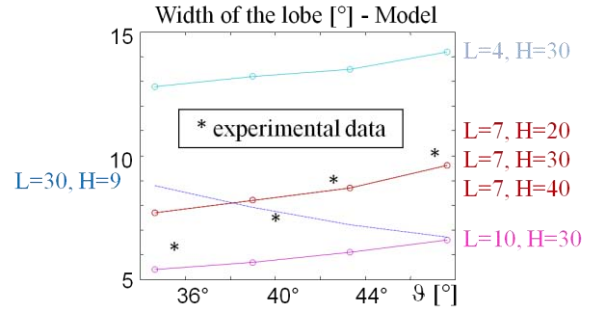


Figure 6. Dihedral basis can be estimated by fitting the model. The dihedral height H is not relevant.

In a forest environment the unimportance of the H parameter means that the actual height of a tree poorly affects the double bounce mechanism. It is rather affected by the horizontal size of the dihedral. If on the one hand it appears obvious to relate the height of the dihedral to the height of the trunk, on the other hand the physical meaning of a limited dihedral basis in a forest environment is less obvious. A possible interpretation of such feature involves the extinction of the wave as it passes through the vegetation layer. This interpretation is described in section 5.

5. A POSSIBLE EQUIVALENT EXTINCTION MODEL

In section 4 a simple model of a dihedral has been analyzed in order to interpret the observations associated with the double bounce mechanism. It resulted that the characteristic dimension of the dihedral is its basis rather than its height. A limited dihedral basis means that optical rays cannot bounce too far away from the trunk. Such behaviour has been explained by hypothesizing a particular extinction profile.

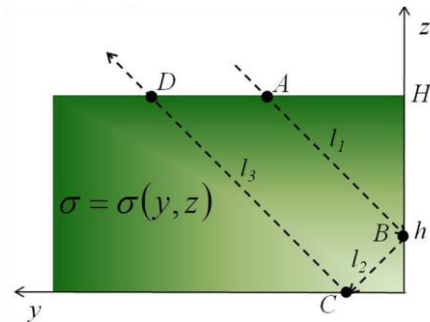


Figure 7. Path travelled by the optical ray through the vegetation layer. The extinction profile (σ) is overlapped.

A vertical extinction profile cannot explain such behaviour as the attenuation is the same for rays bouncing close or far from the trunk. On the contrary by hypothesizing an horizontal extinction profile the situation can be reproduced. In particular we imagined a linearly varying extinction, growing with the distance

from the trunk. In this case the attenuation of each optical ray grows with the elevation of the bounce on the trunk (h), that is with the distance from the tree as shown in equation 2:

$$I_l = \frac{2H}{\cos \vartheta} \sigma_0 + \frac{\tan^2 \vartheta}{\sin \vartheta} (H^2 + h^2) \sigma_1 \quad (2)$$

where I_l represents the intensity associated with the optical ray and σ_0 and σ_1 parameterize the extinction profile according to:

$$\sigma(y, z) = \sigma(y) = \sigma_0 + \sigma_1 y \quad (3)$$

being y the horizontal coordinate as shown in fig. 7. According to this extinction profile, rays bouncing too far away from the trunk experience a strong attenuation thus resulting in a short dihedral basis as required by the model in section 4.

6. CONCLUSIONS

In this paper an analysis of the scattering mechanisms occurring when imaging a forest has been carried out. SAR tomography has been exploited to focus on specific elevation inside the vegetation layer; polarimetry has been used to achieve a physical characterization of the scattering mechanisms. In particular the tomographic algorithm here adopted does not rely on any model of the forest backscattering. It rather exploits the geometrical relationship between the multi baseline signal and the vertical reflectivity profile. Experimental results showed that the ground topography can strongly affect the radar backscatter even in case of a very thick tropical forest. Model free SAR tomography has been used to isolate the signal coming from the ground level and to analyze it. For an average look angle of 43° we observed that a ground slope of about 3° is enough to make the double bounce contribution to vanish. By analyzing such behaviour for several look angles we found that the slope required for the double bounce to vanish increases with ϑ . In order to interpret such behaviour, a simple model of dihedral backscattering has been considered. According to such model the dihedral fitting the data has a short basis and an extended height. It follows that the dihedral height cannot be fully illuminated by the optical rays; as a consequence its actual height is not relevant for the determination of the radar backscatter.

By moving from the model to the real world it can be stated that the double bounce - which is the main contribution as long the ground is flat - is poorly affected by the actual height of the trunk. It rather depends on the room in front of the tree where the bounce can take place. A small region around the tree where the double bounce can take place has been successfully modelled by means of a space varying extinction profile.

7. REFERENCES

1. Dobson, M.C.; Ulaby, F.T.; LeToan, T.; Beaudoin, A.; Kasischke, E.S.; Christensen, N., "Dependence of radar backscatter on coniferous forest biomass," *Geoscience and Remote Sensing, IEEE Transactions on* , vol.30, no.2, pp.412,415, Mar 1992
2. Neumann, M.; Saatchi, S.S., "Polarimetric Backscatter Optimization for Biophysical Parameter Estimation," *Geoscience and Remote Sensing Letters, IEEE* , vol.PP, no.99, pp.1,1, 0
3. Neumann, M.; Saatchi, S.S.; Ulander, L. M H; Fransson, J. E S, "Parametric and non-parametric forest biomass estimation from PolInSAR data," *Geoscience and Remote Sensing Symposium (IGARSS), 2011 IEEE International* , vol., no., pp.420,423, 24-29 July 2011
4. Tebaldini, S., "Algebraic Synthesis of Forest Scenarios From Multibaseline PolInSAR Data," *Geoscience and Remote Sensing, IEEE Transactions on* , vol.47, no.12, pp.4132,4142, Dec. 2009
5. Dubois-Fernandez, Pascale; Oriot, Helene; Coulombeix, Colette; Cantalloube, Hubert; Plessis, Olivier Ruault du; Toan, Thuy Le; Daniel, Sandrine; Chave, Jerome; Blanc, Lilian; Davidson, Malcolm, "TropiSAR, a SAR data acquisition campaign in French Guiana," *Synthetic Aperture Radar (EUSAR), 2010 8th European Conference on* , vol., no., pp.1,4, 7-10 June 2010
6. Reigber, A.; Moreira, A., "First demonstration of airborne SAR tomography using multibaseline L-band data," *Geoscience and Remote Sensing, IEEE Transactions on* , vol.38, no.5, pp.2142,2152, Sep 2000
7. Tebaldini, S.; Rocca, F., "On the impact of propagation disturbances on SAR Tomography: Analysis and compensation," *Radar Conference, 2009 IEEE* , vol., no., pp.1,6, 4-8 May 2009
8. Mariotti d'Alessandro, M.; Tebaldini, S., "Phenomenology of P-Band Scattering From a Tropical Forest Through Three-Dimensional SAR Tomography," *Geoscience and Remote Sensing Letters, IEEE* , vol.9, no.3, pp.442,446, May 2012
9. Freeman, A., "Fitting a Two-Component Scattering Model to Polarimetric SAR Data From Forests," *Geoscience and Remote Sensing, IEEE Transactions on* , vol.45, no.8,

pp.2583,2592, Aug. 2007

10. Knott, E., "RCS reduction of dihedral corners," *Antennas and Propagation, IEEE Transactions on* , vol.25, no.3, pp.406,409, May 1977